Article

Simulation of the Embryonic Stage of ZnS Formation from Aqueous Solution

Said Hamad, Sylvain Cristol, and C. Richard A. Catlow

J. Am. Chem. Soc., **2005**, 127 (8), 2580-2590• DOI: 10.1021/ja045274r • Publication Date (Web): 02 February 2005

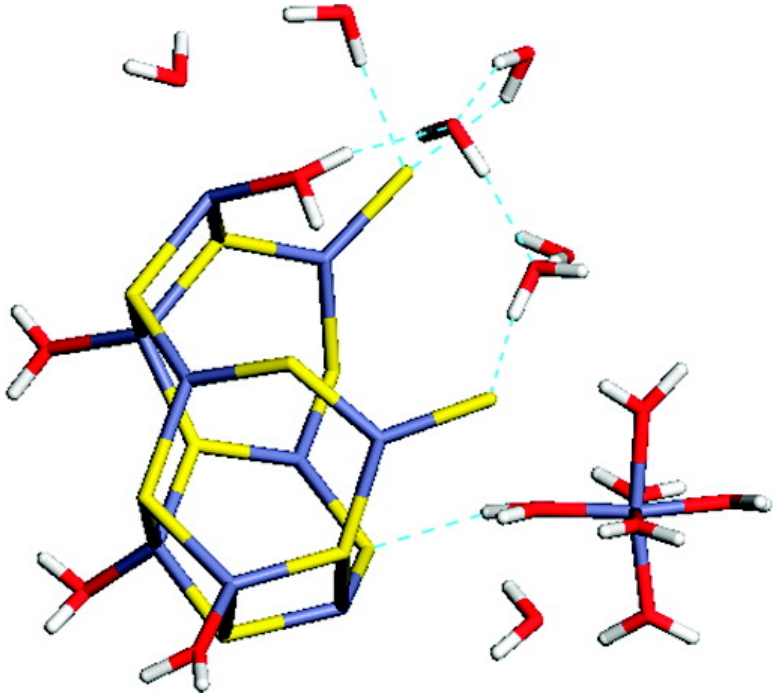

J|A|C|S
ARTICLES
Published on Web 02/02/2005

Simulation of the Embryonic Stage of ZnS Formation from Aqueous Solution

Said Hamad,*,† Sylvain Cristol,†,‡ and C. Richard A. Catlow†

Contribution from the Davy Faraday Research Laboratory, The Royal Institution of Great Britain, 21 Albemarle Street, London W1S 4BS, U.K., and Laboratoire de Catalyse de Lille, UMR CNRS 8010, Bât C3 USTL, F-59655 Villeneuve d'Ascq, France

Received August 5, 2004; E-mail: said@ri.ac.uk

Abstract: We investigate the processes of cluster formation and growth of ZnS from aqueous solution using molecular dynamics simulation techniques. The influence of both temperature and concentration is studied. We show that, at lower temperatures, the crucial process is the transformation of an outer-sphere Zn/S complex to an inner-sphere ion pair. Further growth of the latter is fast to generate negatively charged planar clusters. These clusters interact to form more stable, closed structures, which are found to be the global minima configurations in vacuo. At higher temperatures, no outer-sphere ion pairs are formed, and the larger cluster configurations form much more quickly.

I. Introduction

Nucleation and crystal growth are topics of enduring interest in physical and chemical sciences. Despite the long standing and extensive study and its obvious importance in several fields of science and technology,[1−3] there are many uncertainties in our knowledge of the detailed atomistic mechanisms of nucleation and growth. A major problem with experimental studies is the short time and size scales of nucleation processes. A typical nucleus cluster contains no more than a few hundred atoms, and its appearance is driven by stochastic thermal motion of the atoms; hence, it is not possible to predict when and where it will appear. Furthermore, once the nucleus is formed, it grows very quickly, which prevents the application of many experimental techniques. For these reasons, computer simulations are powerful tools to predict different aspects of both nucleation and crystal growth. Computational techniques can also help to amplify and interpolate experimental observations. Until recently, it was impossible to investigate these subjects due to computer time limitations, but the size and time-scales needed for such simulations are now becoming feasible.[4,5] All of the calculations described in this article have been undertaken using tera-scale computing facilities.

Traditionally, nucleation processes have been explained using what it is now called Classical Nucleation Theory[6−8] (CNT). CNT gives a qualitative explanation of many nucleation events in simple systems (such as nucleation from the melt) but fails to make quantitative predictions, and the introduction of empirical parameters is required. Moreover, in some cases, as in the case of nucleation from solution, CNT gives poor results. A description of the limitations of CNT can be found in ref 9.

One of the most powerful tools in providing information about species in solution and nucleation processes[10] is nuclear magnetic resonance (NMR). For instance, NMR studies[11] show that prenucleation building units of the aluminophosphate ($AlPO_4$−CJ2) appear to generate the crystal structures after undergoing isomerization.

As water is the most important solvent, understanding nucleation from water solution is crucial for many biological and geological processes. Zinc and sulfur are essential in many processes in biological systems,[12] and the mineral forms of ZnS (sphalerite and wurtzite) play an important role in the transport of these two species within the earth. For all of these reasons, a better understanding of the nucleation of ZnS in water is highly desirable.

Several experimental studies have been directed towards that aim.[13−15] EXAFS data suggest[16] the presence of small ZnS particles (<20 nm), with very strong Zn−S bonds, that are not in reversible equilibrium with the solution phase. Electrochemical and spectroscopic experiments[13] show that zinc and sulfide ions in solution initially form pure ZnS clusters, without hydrogen present. For this reason, the approximation we use in

† The Royal Institution of Great Britain.
‡ Laboratoire de Catalyse de Lille.

(1) Boettinger, W. J.; Perepezko, J. H. *Rapidly Solidified Crystallite Alloys*; TMS-AIME: Warrendale, PA, 1985.
(2) Mann, S.; Ozin, G. A. *Nature* **1996**, *382*, 313.
(3) Kulmala, M.; Pirjola, L.; Mäkelä, J. M. *Nature* **2000**, *404*, 66.
(4) Koishi, T.; Yasuoka, K.; Ebisuzaki, T. *J. Chem. Phys.* **2003**, *119*, 11298.
(5) Bartell, L. S. *J. Phys. Chem. A* **2002**, *106*, 10893.
(6) Turnbull, D.; Fisher, J. C. *J. Chem. Phys.* **1949**, *17*, 71.
(7) Buckle, E. R. *Proc. R. Soc. London* **1961**, *A261*, 189.
(8) Oxtoby, D. W. *J. Phys.: Condens. Matter* **1992**, *4*, 7627.
(9) Shore, J. D.; Perchak, D.; Shnidman, Y. *J. Chem. Phys.* **2000**, *113*, 6276.
(10) Haouas, M.; Walspurger, S.; Taulelle, F.; Sommer, J. *J. Am. Chem. Soc.* **2004**, *126*, 599.
(11) Taulelle, F.; Pruski, M.; Amoureux, J. P.; Lang, D.; Bailly, A.; Huguenard, C.; Haouas, M.; Gérardin, C.; Loiseau, T.; Férey, G. *J. Am. Chem. Soc.* **1999**, *121*, 12148.
(12) Pickering, I. J.; Prince, R. C.; Divers, T.; George, G. N. *FEBS Lett.* **1998**, *441*, 11.
(13) Luther, G. W.; Theberge, S. M.; Rickard, D. T. *Geochim. Cosmochim. Acta* **1999**, *63*, 3159.
(14) Zhang, H.; Gilbert, B.; Huang, F.; Banfield, J. F. *Nature* **2003**, *424*, 1025.
(15) Labrenz, M.; Druschel, G. K.; Thomsen-Ebert, T.; Gilbert, B.; Welch, S. A.; Kemmer, K. M.; Logan, G. A.; Summons, R. E.; Stasio, G. D.; Bond, P. L.; Lai, B.; Kelly, S. D.; Banfield, J. F. *Science* **2000**, *290*, 1744.
(16) Helz, G. R.; Charnock, J. M.; Vaughan, D. J.; Garner, C. D. *Geochim. Cosmochim. Acta* **1993**, *54*, 15.

10.1021/ja045274r CCC: $30.25

this work of neglecting water dissociation to form H_3O^+, OH^-, and HS^- complexes in water is unlikely to be significant.

The paper is organized as follows. Section II describes the methodological aspects of our simulations. Section III presents and discusses our results, concentrating first on the development of the potential describing the interaction between ZnS and the water molecules, and second on both NVT and NPT simulations at a variety of temperatures and concentrations, with different starting configurations. Our simulations provide detailed models for the initial stages of the cluster growth process of this material.

II. Computational Details

We study the processes of formation and growth of ZnS clusters in water solution, using molecular dynamics simulations, employing the DL_POLY[17] code. The influence of the temperature and of the solute concentration is investigated by performing simulations at two temperatures (300 and 500 K) and four different concentrations (0.5, 0.75, 1.0, and 1.25 M). The systems consisted of Zn^{2+} and S^{2-} ions randomly placed in a cubic box of $30 \times 30 \times 30$ Å^3 size. The box is then filled with water molecules at the density of liquid water at room temperature (0.977 g/cm^3). Experimental data are usually obtained from solutions with much lower concentrations than those simulated here, but modeling such low concentrations would require very large simulation boxes and would be prohibitively expensive in computer resources. Solutions of the four different concentrations we studied are achieved by having 8, 12, 16, and 20 Zn^{2+} and the same number of S^{2-} ions in the box, plus 818−842 water molecules, depending on the number of ions. The first part of the simulations is a pre-equilibration period of 40 ps, in which the Zn^{2+} and S^{2-} ions are kept fixed and the water molecules are allowed to move. A further 20 ps run of equilibration is then applied, in which all the atoms are free to move. To reduce the effect of the initial configuration, two systems with different initial configurations for each concentration have been investigated. Simulation times range from 1.5 to 6 ns.

The interatomic potentials used to describe Zn−Zn, Zn−S, and S−S interactions have been successfully used previously to model ZnS bulk and surfaces[18] as well as small clusters.[19,20] Interatomic potentials to describe the interaction between ZnS and water molecules[14] have been reported, but they fail to reproduce the values of bond distances and adsorption energies of small clusters obtained with DFT calculations. For this reason, we decided to derive a new set of interatomic potentials giving us the accuracy needed to perform the calculations. The derivation of the potentials is developed in Section IIIa.

The polarizability of the S^{2-} ions is modeled via the shell model of Dick and Overhauser.[21] A positively charged core (bearing all the mass of the ion) is connected to the massless, negatively charged shell by a harmonic spring. In static methods, such as energy minimization, the introduction of the shell model does not bring any complications. In molecular dynamics, however, shells cannot be straightforwardly introduced as they are massless. Two methods have been used to overcome this problem. The first, in the spirit of the Born−Oppenheimer approximation, performs an energy minimization of the shells at each step of the molecular dynamics simulation, so that there are no forces acting on the shells[22] before the next MD step. It would be impractical for us to use this method because it is extremely time-consuming (as several minimization steps are required within each MD step) and it would not allow us to run the nanosecond simulations that are needed in the present study. We therefore opted for the second method, assigning a small mass (0.2 au in our case) to the shells.[23] Unfortunately, this method is also not without problems as there is usually a small transfer of energy from the rest of the system to the core−shell vibrations. For very long calculations, as in the present study, this process could become problematic since the core−shell vibrations can store a large amount of unrealistic kinetic energy. The real physical system would then lose some of its kinetic energy, and ultimately it could freeze. It is possible to solve the problem by introducing an additional thermostat controlling the temperature associated with the core−shell degrees of freedom,[24] but we followed a simpler approach. We introduced a small frictional drag force, b, which varies linearly with the core−shell velocity. The force between a core and shell separated by a distant x becomes now $f_{cs} = {}^1/_2 kx^2 - b\,dx/dt$. The critical value at which the core−shell stops oscillating is $b_{crit} = 462.7$ au/ps. We introduce a friction constant of 15 au/ps, which is only 2% of the critical value. As a result, the polarizability of the S^{2-} ion is properly described, while the core−shell temperature is maintained constant at a low level. We made the necessary changes in the DL_POLY code to include the frictional term. This friction force might induce a loss of energy of the system. To minimize this undesirable effect, we chose to use the Gaussian isokinetic thermostat[25−27] to maintain the room temperature during the simulations, in which the total energy is not constant, but allowed to change in order to maintain a constant temperature. The time step used in these simulations must be small, 0.3 fs, to model correctly the fast vibrations of the shells, caused by their small mass.

III. Results and Discussion

(a) Potential Parameter Derivation. To derive a potential for water interacting with ZnS, we computed the adsorption energy of water molecules on different ZnS clusters using the density functional theory scheme implemented in the Dmol^3 code.[28,29] We used a double numerical basis set and polarization functions, which were introduced to account for sulfur polarizability. The Kohn−Sham equations are solved using the gradient-corrected functional of Perdew et al.[30,31] The geometries of the ZnS clusters as well as the ones of the complex (cluster + water molecules) were fully relaxed, and the interaction energy (E_{int}) is defined as the energy of the complex minus the energy of the free molecules.

To obtain reliable and transferable parameters, we selected the clusters with different Zn coordination, as presented in Figure 1. Two different binding modes were found depending on the charge of the initial cluster. Negatively charged clusters (e.g., ZnS_2^{2-}) bind water through hydrogen bonding between the sulfur atom and the hydrogen atom of the water molecule, although this adsorption mode is found to be unstable for neutral clusters; on the latter, water binds through an interaction between the zinc atom and the oxygen atom of the molecule. Once these interaction energies and geometries have been computed, we may fit then the potential parameters describing the interaction between ZnS and water, using the GULP[32] code. We used our previously developed interatomic potential for ZnS[18] and the

(17) Smith, W.; Forester, T. R. *J. Mol. Graphics* **1996**, *14*, 136.
(18) Hamad, S.; Cristol, S.; Catlow, C. R. A. *J. Phys. Chem. B* **2002**, *106*, 11002.
(19) Spanó, E.; Hamad, S.; Catlow, C. R. A. *J. Phys. Chem. B* **2003**, *107*, 10337.
(20) Spanó, E.; Hamad, S.; Catlow, C. R. A. *Chem. Commun.* **2004**, 864.
(21) Dick, B. G.; Overhauser, A. W. *Phys. Rev.* **1958**, *112*, 90.
(22) Lindman, P. J. D.; Gillan, M. J. *J. Phys.: Condens. Matter* **1993**, *5*, 1019.
(23) Mitchell, P. J.; Fincham, D. *J. Phys.: Condens. Matter* **1993**, *5*, 1031.
(24) Lamoureux, G.; Roux, B. *J. Chem. Phys.* **2003**, *119*, 3025.
(25) Evans, D. J.; Morris, G. P. *Comput. Phys. Rep.* **1984**, *1*, 297.
(26) Evans, D. J.; Hoover, W. G.; Failor, B. H.; Moran, B.; Ladd, J. C. *Phys. Rev. A* **1983**, *28*, 1016.
(27) Evans, D. J. *J. Chem. Phys.* **1983**, *78*, 3297.
(28) Delley, B. *J. Chem. Phys.* **1990**, *92*, 508.
(29) Delley, B. *J. Chem. Phys.* **2000**, *113*, 7756.
(30) Perdew, J. P.; Chevary, J. A.; Vosko, S. H.; Jackson, K. A.; Pederson, M. R.; Singh, D. J.; Fiolhais, C. *Phys. Rev. B* **1992**, *46*, 6671.
(31) Perdew, J. P.; Wang, Y. *Phys. Rev. B* **1992**, *45*, 13244.
(32) Gale, J. D. *J. Chem. Soc., Faraday Trans.* **1997**, *93*, 629.

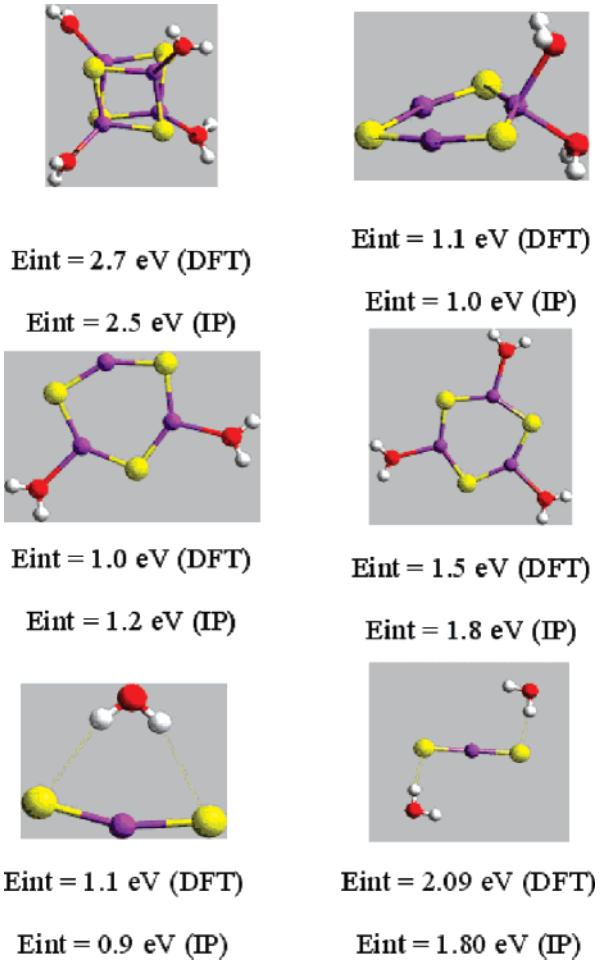

Figure 1. Geometry of hydrated ZnS used for potential derivation, showing the computed DFT interaction energies as well as the interaction energies obtained with the interatomic potential (IP) derived.

consistent valence force field (CVFF) water model,[33] in which the O and H atoms are modeled by point charges, connected through two and three-body forces; the model has been extensively used and validated.[34,35] The interaction between the water molecules and the ZnS clusters was modeled using two Buckingham potentials (Zn−O and S−O). A Lennard-Jones potential with a small A (repulsive) term and a zero B (attractive) term was included between the hydrogen atom of the water molecules and the sulfur atom; it does not, however, significantly influence the computed energies. It has been introduced to improve the stability of the MD simulations by avoiding excessively close approaches of hydrogen to the sulfur atoms. The parameters summarized in Table 1 are the best compromise we found between a good reproduction of the interaction energies and reproducing the correct Zn−O and H−S distances in the complexes.

We emphasize that this set of parameters allows us to describe, with acceptable accuracy, the coordination of one Zn in a variety of environments, namely, with two sulfurs bound to water molecules, with two sulfurs and one water molecule, with two sulfurs and two water molecules, and with three sulfurs

Table 1. Values of the Parameters Fitted to Model the Interaction between ZnS and Water Molecules[a]

	A (eV)	*ρ* (Å)	*C* (eV Å^6)
	Buckingham		
S−O_w	123571	0.25	0
Zn−O_w	125	0.4	0.1
	A (eV Å^{12})[b]	B	
	Lennard-Jones		
S−H_w	3.5	0	

[a] Water−water interaction is modeled using CVFF interatomic potentials. [b] From ref 12.

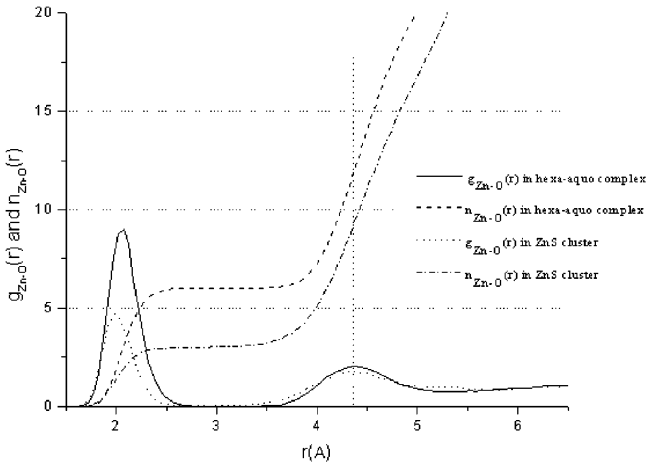

Figure 2. Zn−O RDFs and coordination numbers in two different configurations: Zn in a $Zn(H_2O)_6^{2+}$ complex and in a ZnS cluster. The coordination number in the latter case shows that a $ZnS(H_2O)_3$ complex is formed.

and one water molecule. The results obtained in MD simulations with this set of parameters should, therefore, be reliable as most of the possible coordination possibilities for ZnS clusters in solution are represented. No data concerning the solvation of a single Zn^{2+} ion in solution have been introduced in the fitting procedure. It will be seen in the next section, however, that the correct octahedral coordination is obtained for Zn^{2+} in water with a distance of 2.07 Å between the ion and the water molecules, in good agreement with available experimental data.[36] The interatomic potential we have developed is thus versatile enough to accommodate different coordination spheres around the Zn^{2+} ion.

(b) NVT Simulations at 300K. The first sets of simulations were performed in the NVT ensemble at room temperature. During the equilibration period, the hydration spheres around the Zn^{2+} and S^{2-} ions are formed. The water molecules of the $Zn(H_2O)_6^{2+}$ complex have a strong interaction with the Zn^{2+} cation. We did not observe any exchange of water molecules between the first and second hydration spheres during the simulations, which is consistent with the experimental value[37] of the residence time of 3×10^{-8} s. Figure 2 shows the Zn−O radial distribution function (RDF) and coordination number of the Zn^{2+} cation in a $Zn(H_2O)_6^{2+}$ complex. There is a prominent peak at 2.07 Å, which corresponds to the positions of the oxygen atoms in the first coordination shell of the hexa−aquo complex. The second coordination shell is less clearly defined since its

(33) Lau, K. F.; Alper, H. E.; Thacher, T. S.; Stouch, T. R. *J. Phys. Chem.* **1994**, *98*, 8785.
(34) Oliveira, C. A. F.; Guimaraes, C. R. W.; Alencastro, R. B. *Int. J. Quantum Chem.* **2002**, *90*, 786.
(35) Helms, V.; Wade, R. C. *J. Comput. Chem.* **1997**, *18*, 449.
(36) D'Angelo, P.; Barone, V.; Chillemi, G.; Sanna, N.; Meyer-Klaucke, W.; Pavel, N. V. *J. Am. Chem. Soc.* **2002**, *124*, 1958.
(37) Miyanaga, T.; Sawa, Y.; Sakane, Y.; Watanabe, I. *Phys. Rev. B: Condens. Matter* **1995**, *208−209*, 393.

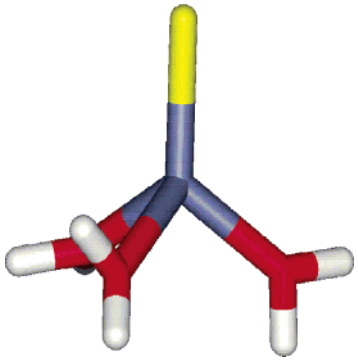

Figure 3. Structure of the ZnS cluster, which is bound to three water molecules and forms a $ZnS(H_2O)_3$ complex. Yellow stick represents S; blue stick represents Zn; red sticks represent O; and white sticks represent H. The same color code applies to all figures.

associated peak is smaller and it spreads over a broader region, from 4.2 to 4.7 Å. The maximum in this second peak is at 4.38 Å, with a coordination number of 12.3.

S^{2-} anions do not form a stable complex with the water molecules since the interaction with them is weaker. They interact with 8−12 water molecules in the first hydration shell (the S−O RDF can be seen in the Supporting Information), but the residence time is very short and they are constantly being replaced by molecules from the second hydration shell. Zn^{2+} and S^{2-} anions eventually interact to form a ZnS cluster, for which the time necessary depends on the concentration of the solution. The gain in energy accomplished by the formation of this ZnS bond from a $Zn(H_2O)_6^{2+}$ complex and a S^{2-} anion in water solution is -164 kJ·mol^{-1}. This value is calculated using two simulations: one with a ZnS cluster in water, and another in which the two ions are separated. The Zn−O RDF and coordination numbers of a Zn atom in a ZnS cluster are plotted in Figure 2, clearly showing that the number of water molecules in the first hydration shell reduces to three. As can be seen in Figure 3, the oxygen atoms interacting with a ZnS cluster occupy three vertexes of a tetrahedron and the S atom occupies the fourth.

Despite the thermodynamic driving force, there is an energy barrier opposing the formation of a ZnS cluster from a $Zn(H_2O)_6^{2+}$ complex and a S^{2-} anion. There is a strong electrostatic attraction between Zn^{2+} and S^{2-}, but the hydrated Zn^{2+} is also strongly bound to the water molecules. An outer-sphere complex is then formed in which the $Zn(H_2O)_6^{2+}$ complex remains, in fact, with the S^{2-} ion at a distance of 4.6 Å (Figure 4). The S^{2-} anion is situated on top of one of the faces of the octahedron formed by the $Zn(H_2O)_6^{2+}$ complex. The three water molecules forming the face have a hydrogen atom each pointing toward the S^{2-} anion, therefore maximizing the interaction and providing the most stable configuration for the outer-sphere ion pair. However, there is another configuration in which the S^{2-}, the Zn^{2+}, and one water molecule lie in the same straight line. In this case, the S^{2-} anion interacts with only one water molecule, and the distance to the Zn^{2+} is 5.2 Å larger than that in the other case, due to the presence of the water molecule between them. Ion pairs mainly adopt the first configuration, which is the most stable, but there will be a smaller equilibrium concentration of the less-stable configuration, creating the small shoulder at 5.2 Å observed in the Zn−S RDFs. Ion pairs are stable units at room temperature; they move through the liquid water without dissociating for hundreds of

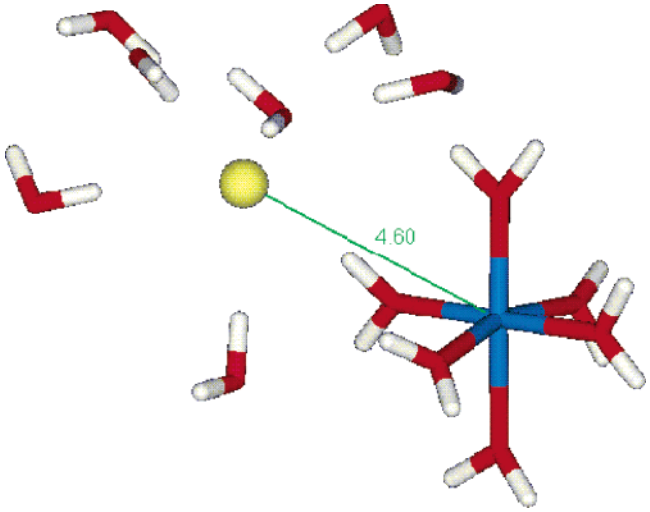

Figure 4. Snapshot of an ion pair with water molecules surrounding the S^{2-} ion. The ion pair is formed by the $Zn(H_2O)_6^{2+}$ complex and the S^{2-} ion, attracted by Coulombic forces. They move through the liquid with an average distance of 4.6 Å. Zn^{2+} and S^{2-} do not immediately form a cluster, owing to the presence of the six water molecules strongly bound to the Zn.

picoseconds. A Zn^{2+} ion can be part of more than one ion pair since two ion pairs can interact to form a larger entity in which the Zn^{2+} cations stay in their hexa−aquo complexes while the S^{2-} anions oscillate at 4.6 Å from the Zn^{2+} atoms.

As a result, a network of ion pairs is formed, involving most of the Zn^{2+} and S^{2-} ions and creating areas with high concentrations of solute separated from areas in which no solute is present. Studies in different systems suggest that this phase separation might be the first stage of the nucleation process.[9,38,39] It was observed in all of our simulations at room temperature, regardless of the concentration.

We proceed now to give the detailed results obtained for each concentration derived from the NVT simulations at 300 K.

0.5 M Concentration. Figure 5 shows the change with time of the Zn−S RDFs for all four concentrations simulated for 1.5 ns. The associated coordination numbers are available as Supporting Information. The RDF for the lowest concentration after 50 ps is flat, showing that there is very little order (due to the random initial distribution of the ions), and no ion pairs are formed yet. After 500 ps, we observe a small broad peak at ∼4.6 Å, corresponding to the ion pair Zn−S distance. At 1 ns, we see a sharp peak appearing at 2.1 Å, which is the Zn−S distance in a ZnS pair, indicating that the activation energy for breaking the $Zn(H_2O)_6^{2+}$ complex has been overcome to form the pair. Once this cluster is formed, the energy barrier to break it is even larger than that to create it, hence, there is no dissolution of any ZnS cluster in all of the simulations, in agreement with experimental results.[16]

After 1.5 ns, the first peak becomes higher and sharper, indicating that there are more ZnS bonds formed. The system then consists of several ion pairs: a planar $(ZnS_3)^{4-}$ cluster (Figure 6), and three Zn^{2+} ions interacting with the sulfide ions within the cluster.

The processes described above refer explicitly to one of the two NVT simulations performed at 300 K and 0.5 M concentration. However, as noted, we carried out two simulations (with

(38) Anwar, J.; Boateng, P. K. *J. Am. Chem. Soc.* **1998**, *120*, 9600.
(39) Wolde, P. R. t.; Frenkel, D. *Science* **1997**, *277*, 1975.

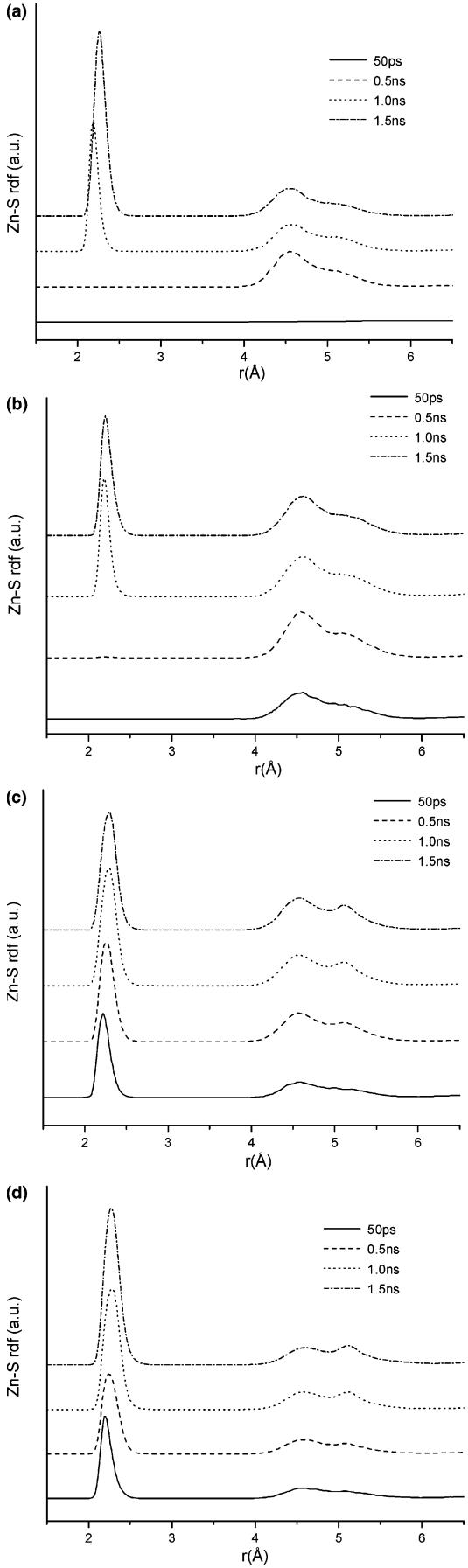

Figure 5. Zn−S RDFs during the simulation, at four different concentrations: (a) 0.5 M, (b) 0.75 M, (c) 1.0 M, and (d) 1.25 M.

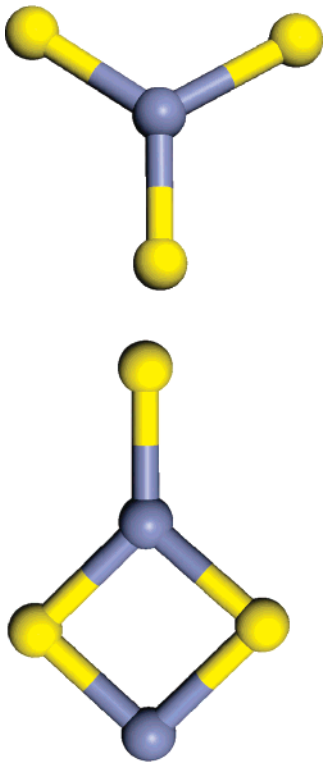

Figure 6. Structure of the two first clusters formed in solution, $(ZnS_3)^{4-}$ and $(Zn_2S_3)^{2-}$.

different initial configurations) at each temperature and concentration to assess the influence that the choice of the random initial configuration has over the final results. It is gratifying that for the other simulation, which is not discussed in detail, the process is similar; even the final cluster is the same. Indeed, in all of the systems studied, the results of the two simulations are similar, with some obvious differences appearing due to the different starting points, but the cluster formation processes show the same general features. We may therefore have reasonable confidence in the generality of our results.

0.75 M Concentration. The RDF of one of the two simulations of 0.75 M systems is shown in Figure 5b. During the first 50 ps, the ion pairs start to form. At 0.5 ns, the network of ion pairs is already created, generating a series of "threads" that expand all across the unit cell. Eventually, some of these ion pairs gain enough energy to overcome the activation barriers and form ZnS bonds, giving rise to the sharp peaks observed in the RDF at 1 and 1.5 ns.

In simulations at 0.5 M, only the $(ZnS_3)^{4-}$ cluster is formed after 1.5 ns, while the rest of the ions are still forming ion pairs. At 0.75 M, we also observe the initial formation of this cluster. Therefore, once a ZnS cluster is formed, it attracts additional S^{2-} ions rather than Zn^{2+} in hexa−aquo complexes and forms first a $(ZnS_2)^{2-}$ cluster; again, this triplet will attract a further S^{2-} to form the $(ZnS_3)^{4-}$ cluster. To understand this behavior, we note that once a ZnS cluster is formed, the very stable hydration shell of six water molecules is broken and the Zn atom is weakly attached to only three water molecules (Figure 4). So when a S^{2-} anion approaches, it will be easier to remove one of these water molecules than one of the water molecules bound to a single Zn^{2+} cation; hence, growth into a $(ZnS_2)^{2-}$ cluster is more facile than dissociation of another hexa−aquo complex.

This feature is general and is observed in all simulations at room temperature. The formation and growth of ZnS clusters does not start as an extended process in which Zn and S atoms from all of the system form small clusters that subsequently aggregate and grow. Rather, it is an activated process, triggered by the rupture of ion pairs. In this sense, it could be argued that the precritical nucleus is a ZnS cluster, because once that cluster is formed, it will start growing. A similar effect has been observed in simulations of the nucleation of AgBr from solution,[9] where the critical cluster size is found to be between 1 and 3 AgBr units. It must be noted that this prenucleus, which enables the initial growth of larger ZnS clusters, is different from the secondary (or even tertiary) nuclei that must appear at a later stage, which initiate the formation of clusters with any of the crystalline polymorph structures. This lack of more adequate definitions for the different nuclei, which have different characteristics, is a consequence of the lack of a nucleation theory able to explain these processes.

The $(ZnS_3)^{4-}$ cluster attracts the positively charged $Zn(H_2O)_6^{2+}$ complexes, which move around it, until one of them overcomes the energy barrier allowing the Zn^{2+} ion to attach to the cluster. A very stable $(Zn_2S_3)^{2-}$ cluster is then formed (Figure 6), which does not grow during the rest of the simulation.

Previous experimental studies[13] of ZnS nucleation from water solution proved that the first stage of the ZnS nucleation is the creation of small clusters of 1:1 stoichiometry, followed by the formation of clusters with 3 S:2 Zn stoichiometry. Although the systems they studied have a much lower concentration, the atomic processes involved must be similar in both cases; therefore, our simulations give insight into the structure of these initial clusters, as well as the path followed in their growth.

1 M Concentration. For this high concentration, the formation of ZnS clusters occurs very quickly. The network of ion pairs occupies a large volume, fluctuating in the entire box, creating regions with high concentrations of ZnS and regions with only water. Figure 5c shows the RDF of one of the 1 M systems. In the first 50 ps, the peak associated with the ion pair network is already formed, as well as the peak associated with ZnS clusters. After 0.5 ns, ZnS and $(ZnS_3)^{2-}$ clusters appear. The same physical reasons that make these two small clusters more likely to bind extra atoms than isolated ions also make them more likely to come together and form a $(Zn_2S_4)^{4-}$ complex, which happens before 1 ns of simulation. This cluster does not undergo further growth in the next 0.5 ns. No other ion pair is broken to form a ZnS cluster in that period, as can be noted from the RDF. Figure 7 shows a snapshot of the system at 1.5 ns. It is interesting to note the clear distinction between the regions of high and low ZnS concentration. $Zn(H_2O)_6^{2+}$ complexes have a stronger interaction with isolated S^{2-} ions (forming ion pairs) than with large clusters, such as $(Zn_2S_4)^{4-}$. For this reason, the latter are pushed away from the region of high ZnS concentration, as can be seen in the figure, a factor that slows down the process of cluster growth.

1.25 M Concentration. The behavior of the system at this high concentration is somewhat different from that at lower concentrations. As in the case of 1.0 M concentration, ZnS units are rapidly formed, which now, however, happens in many places simultaneously. As a result, the RDF (Figure 5) shows the first peak even before the network of ion pairs has been

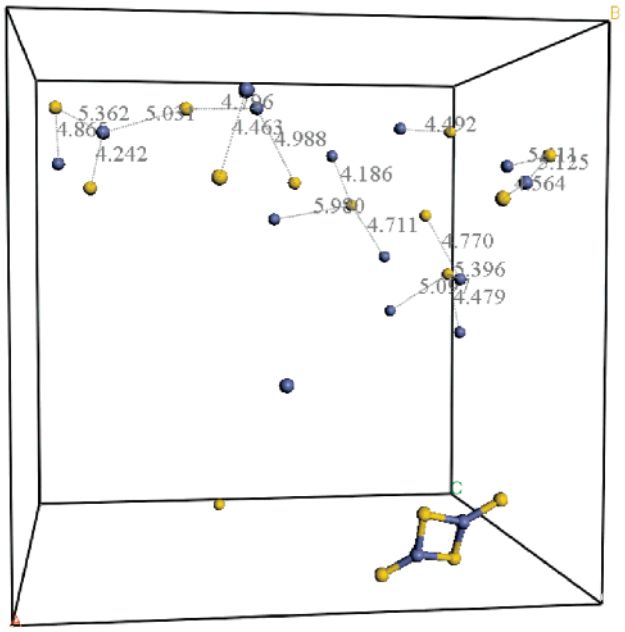

Figure 7. Snapshot of the system with 1.0 M concentration at 1.5 ns. Water molecules have been removed to allow a clear view of the Zn and S atoms. The distances between atoms forming ion pairs are shown. Note the wide range of distances over which the ion pairs exist, vibrating around the energy minimum at 4.6 Å.

formed. These clusters aggregate to form larger clusters, such as the previously described $(Zn_2S_3)^{2-}$ and $(Zn_2S_4)^{4-}$ species. However, the most interesting result from the simulation at high concentrations is that we can see the creation of large clusters, which would require much longer simulation times to be observed at low concentrations. In one of the simulations, two $(Zn_2S_4)^{4-}$ clusters are formed and coexist for a while. During the simulation, they interact with the same $Zn(H_2O)_6^{2+}$ complex, which stays between them. Thermal motion eventually provides sufficient energy to break the complex, and the Zn^{2+} sticks to one of the clusters. Once the complex is broken, the other $(Zn_2S_4)^{4-}$ cluster is able to stick to the same Zn^{2+} ion, forming a large $(Zn_5S_8)^{6-}$ cluster, which has an almost linear structure. The large negative charge of that cluster causes another Zn^{2+} to be attracted to form $(Zn_6S_8)^{4-}$, which has a very unstable initial configuration, but undergoes a structural rearrangement to achieve the stable structure shown in Figure 8. The striking characteristic of the latter cluster is that it does not have four coordinated atoms. Zn atoms have a higher coordination number than S atoms, but they are only two- or three-coordinated. *Ab initio* and interatomic potential-based calculations[19,40] have proved that the minimum energy structures for $(ZnS)_n$ clusters, with $n = 6-47$, are the so-called "bubble clusters", spheroidal structures composed of the arrangement of squares (Zn_2S_2 rings) and hexagons (Zn_3S_3 rings), in which all of the atoms are three-coordinated. It is not surprising then that nonstoichiometric clusters, such as the ones we show here, also have three-coordinated atoms. The $(Zn_6S_8)^{4-}$ cluster has two squares and two hexagons, which are the structural units of the bubble clusters.

(c) NPT Simulations at 300 K. The NVT simulations described in the previous section use a very small time step. For this reason, the simulations are very time-consuming, with

(40) Matxain, J. M.; Fowler, J. E.; Ugalde, J. M. *Phys. Rev. A* **2000**, *61*, 053201.

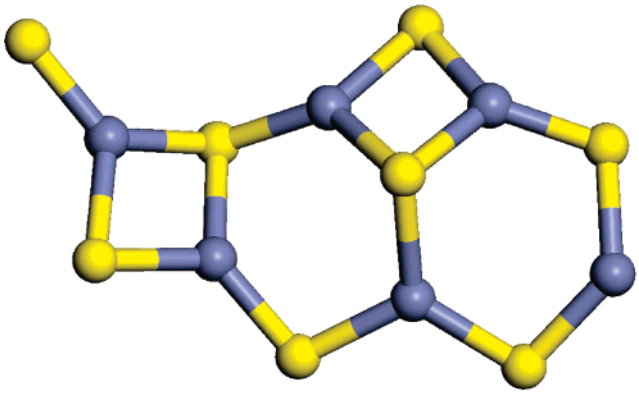

Figure 8. $(Zn_6S_8)^{4-}$ cluster formed after 1.5 ns simulation in the system with 1.25 M concentration. The structure is close to planar, and its building units are squares and hexagons, the same building units of the bubble clusters that are the most stable structures of $(ZnS)_n$ clusters in vacuo for $n = 10-47$.

long calculations needed to simulate relatively short times. The need to break very stable ion pairs in order to permit cluster growth makes the calculations even longer and more time-consuming. In view of the large amount of computer time needed to perform these simulations, we decided to take a new approach. The influence of the atomic polarizability on the processes of ion aggregation seems to be small. We therefore decided to model the S^{2-} ions as rigid rather than polarizable ions, enabling an increase in the time step up to 1 fs that allows us to make a more efficient use of the computer time. We also considered that there could be significant volume changes due to the changes in the hydration spheres when the clusters grow, which would be better modeled in the NPT ensemble, where the Nosé−Hoover[41,42] thermostat and barostat are used to maintain the system at room temperature and pressure. With these changes, we are able to simulate the systems for 6 ns, which allows us to gain further insight into the nucleation process.

At 0.5 M Concentration. In one of the two simulations at this concentration, we do not see the formation of any ZnS cluster; all ions stay in solution during the entire 6 ns, indicating the high stability of the ion pairs and the large energy barrier that prevents their rupture. In the other simulation, a $(Zn_2S_4)^{4-}$ cluster, like that shown in Figure 7, is formed, confirming that when an ion pair is broken to form a ZnS cluster, this cluster undergoes further growth quickly.

At 0.75 M Concentration. Systems at this concentration form larger clusters than at 0.5 M. The process of cluster formation is easier to understand through the use of schematic figures, as in Figure 9. During the first nanosecond, the clusters that are formed are the usual ones that start cluster growth: $(ZnS_2)^{2-}$ and $(ZnS_3)^{4-}$. After 1.6 ns, a cluster is formed with a structure that is very representative of the way in which nucleation of ZnS occurs. The $(Zn_3S_6)^{6-}$ cluster has a planar, hexagonal-like structure, which is one of the building units of the bubble clusters. It is also a building unit of larger planar clusters, such as that in Figure 8. The subsequent addition of a $(ZnS_2)^{2-}$ cluster generates a species with a high negative charge, which is very unstable and needs to attach another Zn^{2+} cation in order to undergo a transformation and gain a stable configuration,

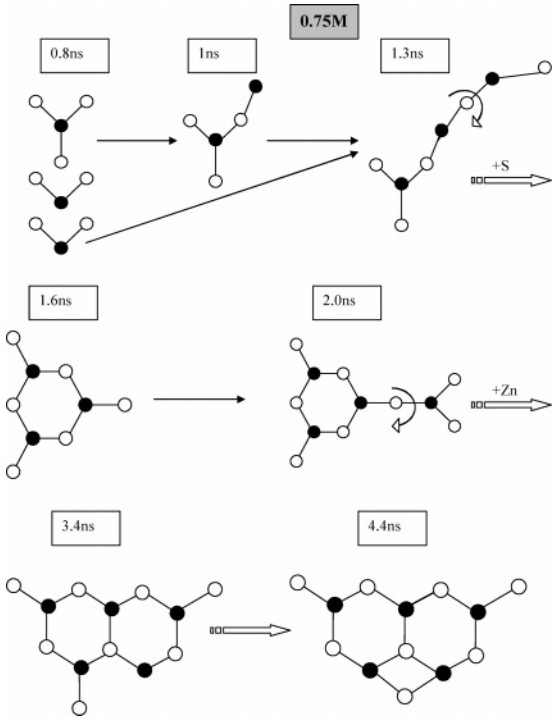

Figure 9. Schematic representation of the cluster formation process. Black circles represent Zn atoms; white circles represent S atoms, and gray circles represent Zn atoms coordinated to four S atoms in a tetrahedral arrangement. Bonds crossed by a semicircular arrow have freedom to rotate. This figure shows the results of one of the two systems simulated at 0.75 M. (The same color codes and representations apply to the rest of the figures from Figures 10−14, at the concentrations indicated.)

consisting of two planar hexagons sharing an edge. After 1 ns, one S atom forms a new bond bridging two Zn atoms, creating a square. As a result, the structure is no longer planar. An arrangement of hexagons alone would not be able to form a closed structure; they can only form planes (as in the graphite structure). Indeed, as discussed in ref 19, Euler's law states that it is necessary to have 6 squares in order to bend the structure and enclose a volume. So the addition of squares to an arrangement of hexagons bends the structure; the more squares present, the more bent it will be. After 4.4 ns, no more changes of the cluster are observed.

Figure 10 shows the behavior of the other system studied with a 0.75 M concentration. The most remarkable feature is the appearance of clusters with four coordinated atoms. After 1.2 ns, a $(Zn_3S_5)^{4-}$ cluster is formed in which a Zn atom is surrounded by four S atoms placed at the vertices of a tetrahedron, which is the local environment of Zn atoms in the bulk phases of ZnS. However, the structure is only transient, and when a new Zn atom is attached, the cluster is transformed to one with a planar structure comprising a hexagon and a square sharing one edge. Therefore, the presence of a Zn ion with the tetrahedral structure of the bulk is not sufficient to nucleate the crystal formation and induce the clusters to grow as bulklike structures. The clusters present in the initial stages of crystal growth are preferentially planar; four coordinated atoms are only transient structures that easily evolve and become three coordinated.

At 1 M Concentration. The two systems with 1 M concentration have similar behavior (see Figures11 and 12). Although formed at different times, the final clusters in both systems are $(Zn_2S_4)^{4-}$ and $(Zn_3S_6)^{6-}$. The main difference

(41) Hoover, W. G. *Phys. Rev. A* **1985**, *31*, 1695.
(42) Melchionna, S.; Ciccotti, G.; Holian, B. L. *Mol. Phys.* **1993**, *78*, 533.

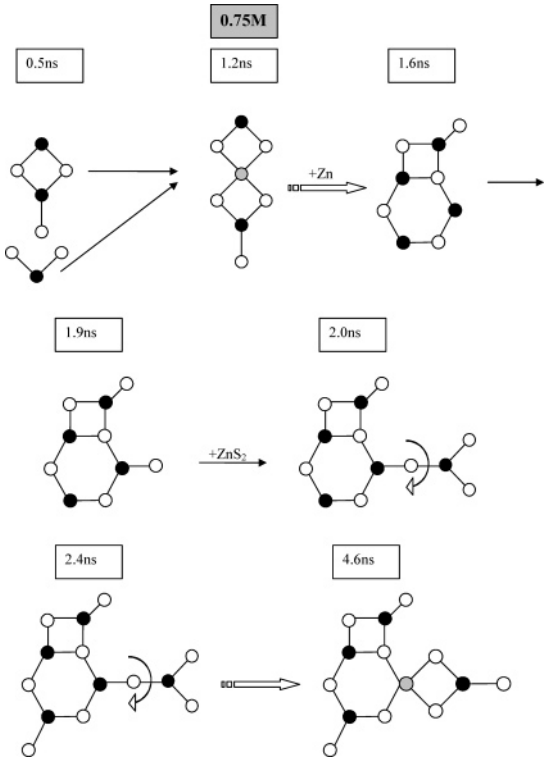

Figure 10. Schematic of one of the growth sequences at 0.75 M.

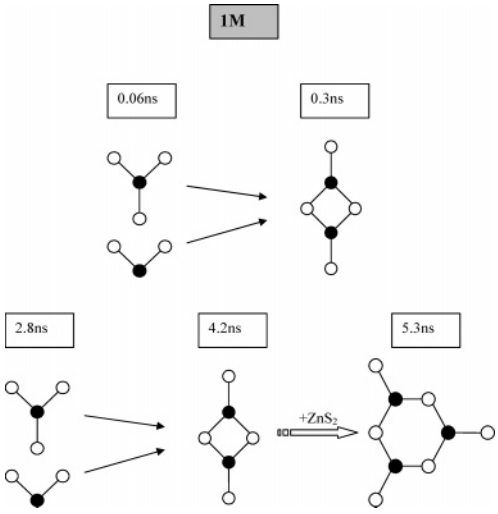

Figure 11. Schematic of one of the growth sequences at 1 M.

between them is that in one case, the $(Zn_3S_6)^{6-}$ cluster has a planar structure, while in the other, there is a four-coordinated Zn atom with tetrahedral arrangement. The difference in total energy between the two structures shows that this nonplanar structure is more stable than the planar one by 0.1 eV, so if the simulation was longer, we could see the cluster jumping the energy barrier to undergo a structural transformation and become nonplanar. However, as seen for the systems with a 0.75 M concentration, that structure can easily be changed when other atoms are attached and new planar clusters are more likely to be formed.

At 1.25 M Concentration. At this concentration, larger clusters are formed (see Figures13 and 14). $(Zn_3S_6)^{6-}$ clusters are formed at approximately 3 ns in the two systems simulated at this concentration. One of the systems has the planar

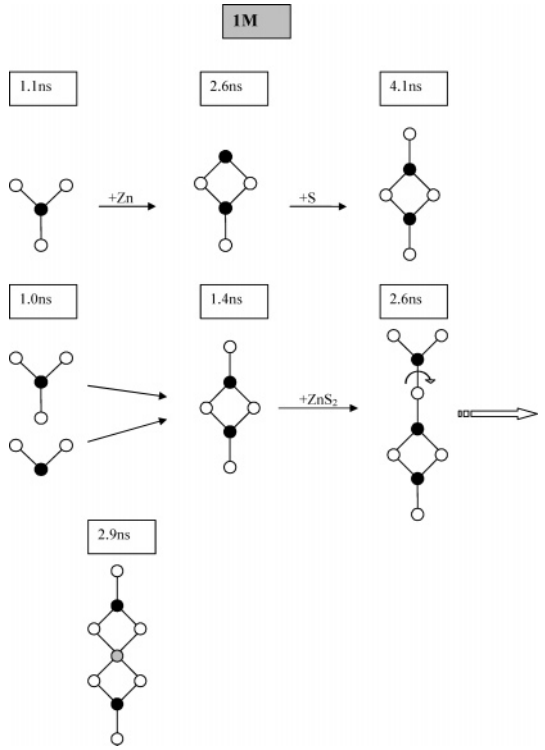

Figure 12. Schematic of one of the growth sequences at 1 M.

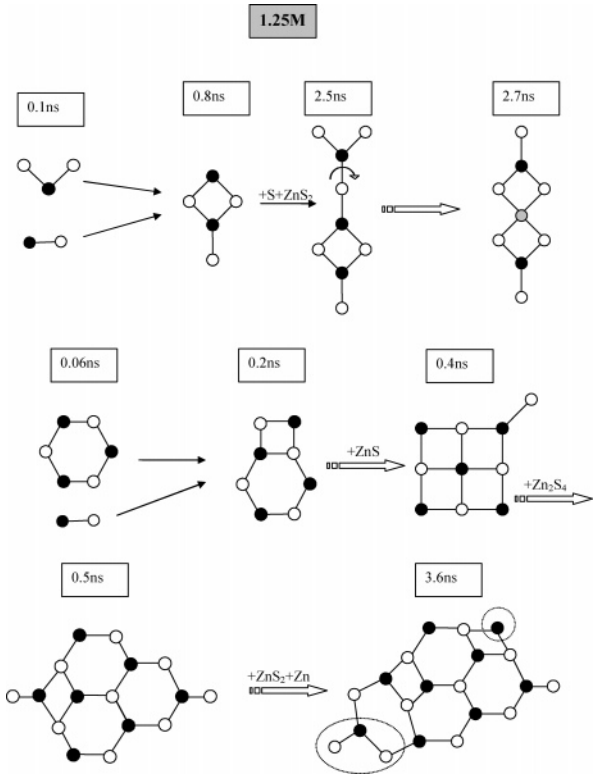

Figure 13. Schematic of one of the growth sequences at 1.25 M.

configuration of the $(Zn_3S_6)^{6-}$ cluster, while the other has the nonplanar configuration. They remain unchanged for the remaining 3 ns of the simulation, indicating that the energy barrier between the two conformations is quite high. More clusters are formed in other regions of the system; most are close to planar structures formed by squares and hexagons. The largest cluster created after 6 ns is shown in Figure 15. It has

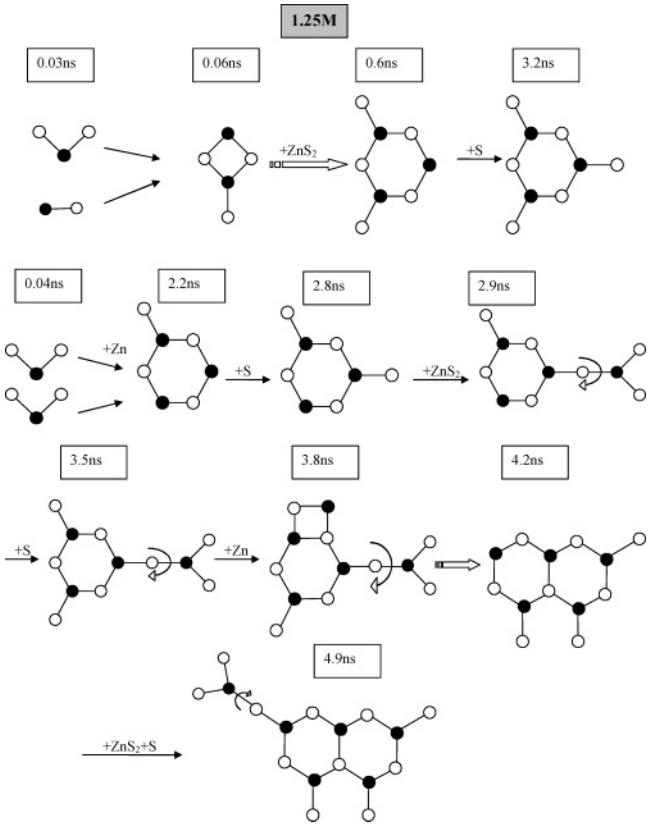

Figure 14. Schematic of one of the growth sequences at 1.25 M.

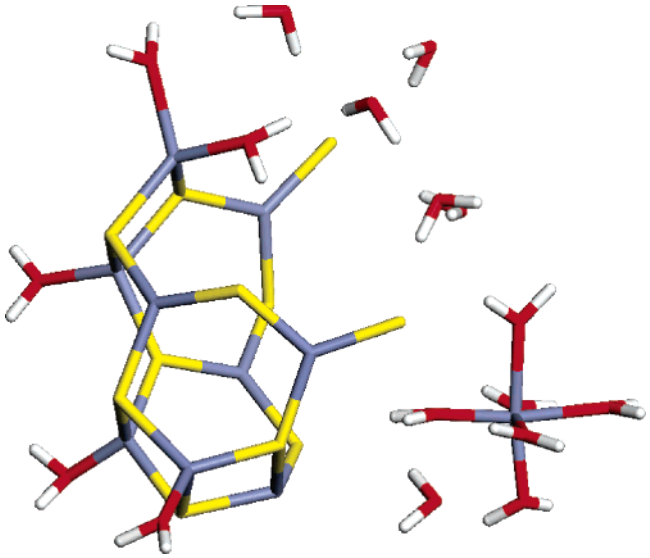

Figure 15. $(Zn_9S_{11})^{4-}$ cluster formed after 6 ns simulation in the system with 1.25 M concentration. The structure is nonplanar, due to the presence of three squares, making it similar to a bubble cluster. There are no water molecules bound to the internal side of the developing bubble, suggesting that the addition of more atoms would easily form a closed bubble without water inside.

11 S and 9 Zn atoms; there are 4 hexagons and 3 squares. The presence of the 3 squares results in a bent structure, so the cluster has the shape of an open bubble, suggesting that the following step in the nucleation process of ZnS is the creation of closed bubble clusters, which are the most stable structures in vacuo. The open bubble of Figure 15 does not have water molecules in the region that would be the inner region of the bubble, so addition of more atoms would not enclose any water molecules. There are only slight changes in volume in all of the simulations we performed. However, if hollow bubble clusters were created, this would generate an expansion of the system due to the creation of forbidden regions for the water molecules; the larger the bubble, the bigger the expansion. It would be interesting if this effect could be observed experimentally.

As many previous studies have found, the process of nucleation and crystal growth is not as simple as the classical nucleation theory suggests. CNT is based in the assumption that clusters are constantly being formed due to the random thermal motion and redissolved because of the high energy associated with their strained surfaces. It is only when the cluster reaches a certain size that it can continue to grow. As our study suggests, this is not a valid description for all systems. In our case, what it is restraining the cluster growth is the formation of ion pairs, which are very stable units. Once they are broken to form a ZnS cluster, they can undergo further growth much faster, by attracting S^{2-} ions from the solution, which are not strongly attracted to the water molecules. The association of various clusters to form a bigger one is also easier than the breaking of an ion pair. Another reason why CNT would not offer valid predictions for our system is because we do not see formation and dissolution of clusters; when a Zn^{2+} and a S^{2-} come together, they form strong bonds, which are not broken during the time of the simulation (which agrees with experimental data[16]). The present and other studies suggest that it is necessary to modify the CNT, or perhaps to create a completely new theory of nucleation, able to account for systems such as ZnS. This new nucleation theory would have to take into account the two stages in which the formation of small clusters occurs: the first in which the atoms do not interact strongly, dominated by the presence of ion pairs; the second, when ZnS clusters are formed. Although these two stages are still far away from the formation of crystal-like structures, they must be taken into account in any theory because they determine the rate of creation of the units that will eventually grow into crystals.

(d) NVT Simulations at 500 K. To assess the influence of temperature on our system, we decided to perform simulations at the higher temperatures of 500 K. Due to the increase in ion velocities at this temperature, we do not need very long simulations to observe the initial stages of cluster growth, so we simulated the systems for 0.5 ns. Polarizability via the shell model is included for the S^{2-} ions, and the Evans[25−27] thermostat is used. The volume of the systems is the same as that in the NVT calculations at 300 K since we wished to ensure that any difference between the two simulations was caused only by the difference in temperature.

The main difference between the simulations at 300 and 500 K is that at high temperatures, there are no ion pairs created; $Zn(H_2O)_6^{2+}$ complexes are formed, but the kinetic energy of the other water molecules is high enough to break them and there is a constant exchange of water molecules between the first hydration shell and the rest of the liquid.

We observed earlier that the existence of stable ion pairs and the necessity of breaking them were the main factors limiting the formation of ZnS clusters. Since there are no ion pairs at 500 K, the process of cluster growth is much faster. After a few picoseconds of simulation, we see the formation of several ZnS and $(ZnS_2)^{2-}$ clusters, which occurs in all of the systems

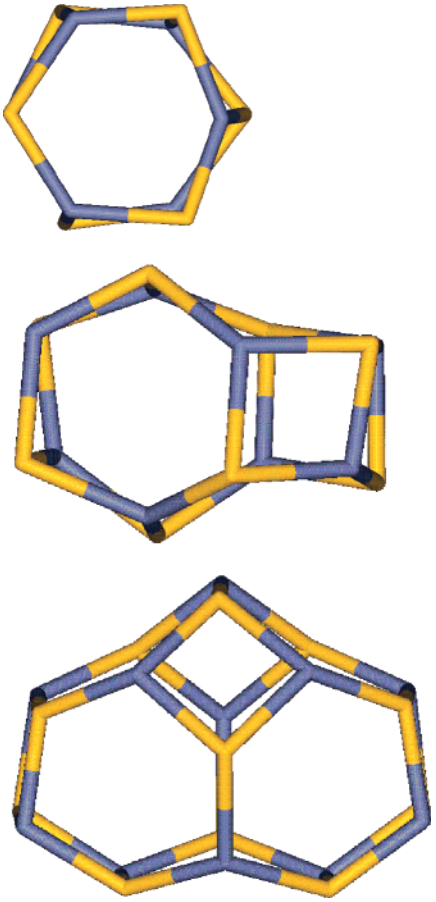

Figure 16. Structures of clusters formed in the calculations at 500 K. The thermal motion at this high temperature induces jumps over energy barriers, and bubble clusters are formed faster than at 300 K.

studied, regardless of the concentration. Unlike the case of 300 K (in which higher concentrations allowed a faster growth due to the higher probability of breaking ion pairs), at 500 K, there are no significant differences in the rate at which clusters are formed for the different concentrations because every time a Zn^{2+} approaches a S^{2-}, a new bond is created. The aggregation process is therefore only limited by the ionic diffusion rates.

The small clusters formed at the beginning have the same structures as those at 300 K: $(ZnS_2)^{2-}$, (Zn_2S_2), $(Zn_2S_3)^{2-}$, etc. The only one that does not appear at 500 K is the highly charged $(ZnS_3)^{4-}$; most of the S atoms are already attached to other Zn atoms, so there is only a small chance that a $(ZnS_2)^{2-}$ cluster finds an isolated sulfur ion. The differences between the two temperatures become more apparent for larger clusters. At 300 K, we saw that the structures are mainly planar, with very few closed configurations. At 500 K, the atoms have more kinetic energy, which allows them to jump the energy barriers between different conformations; hence, the lower-energy configurations are found more easily. We therefore see the formation of several clusters that are also found to be the global minima structures in vacuum (Figure 16).

Clusters, however, do not always grow through a succession of minima. Sometimes the process is so fast that a cluster does not have enough time to rearrange and find the minimum before more atoms are attached to it, which happens, for example, in the calculations with high concentrations (i.e., 1 and 1.25 M), where the final states are very disordered clusters containing all of the ions in the simulation; large clusters are formed, with a bubble-like region, while in other regions, there are four coordinated atoms. For low concentrations, the total number of ions is small, which makes it easier to find the global minima, and the final structures are bubble clusters with only three coordinated atoms.

IV. Summary and Conclusions

Our molecular dynamics simulations have given a new insight into the initial stages of cluster growth of ZnS in water solution. At room temperature, Zn^{2+} ions interact with six water molecules to form very stable $Zn(H_2O)_6^{2+}$ complexes. These complexes attract by Coulomb forces the S^{2-} ions in solution (which do not form stable complexes) and form ion pairs. Ion pairs are stable units, with a mean Zn−S separation of 4.6 Å. To form a ZnS cluster, the aqueous complex of a Zn^{2+} ion must be broken. As the process has an appreciable activation energy barrier, the creation of ZnS clusters is relatively slow. Since S^{2-} ions can be part of more than one ion pair, a network of ion pairs is formed, creating regions of high and low concentrations of ZnS. Eventually, some atoms jump the barrier and form ZnS clusters, the rate of which, as expected, increases with concentration.

Once a ZnS cluster is formed, it is relatively easy for it to continue growing. Although experimental results are usually obtained for concentrations that are thousands of times lower than the ones we are able to model, it is interesting to note that they suggest that the initial clusters formed have a 1:1 Zn/S stoichiometry, in agreement with our predictions. They also find that the next step is the formation of clusters with a S/Zn ratio of 3/2, which in our simulations, is a planar cluster. These clusters continue growing due to the high concentration of our solutions, so we are not able to elucidate whether these planar clusters are the same predominant units observed experimentally at very low concentration.

As previously shown, using global minimization techniques,[19,40] the most stable structures of $(ZnS)_n$ clusters, with $n = 6-47$, are not bulklike but bubble clusters (hollow clusters) in which all of the atoms are three-coordinated. Our simulations show that the initial ZnS clusters formed in water solutions are not bulklike. We found that they typically form planar structures that can be regarded as components of bubble clusters. When they reach a large size, they begin to bend, acquiring a structure that is even more similar to that of the bubbles. Owing to computer time limitations, we are not able to see the formation of a closed bubble at 300 K, but our calculations suggest that it would be the next step in the nucleation process. The formation of the ZnS crystal structures must therefore be achieved at a later stage.

In summary, the process of ZnS nucleation and crystal growth, predicted from simulations and confirmed in part by experiments, is as follows. First, small ZnS clusters form in solution when ion pairs are broken. These clusters continue growing and become bubble clusters.[19] Bubble clusters continue growing and become double bubbles,[20] which have some four-coordinated atoms. At some stage, a rearrangement of the network of four-coordinated atoms must happen for larger clusters, leading to the creation of the known ZnS crystal phases. Small nanocrystals are more likely to show a wurtzite structure.[43]

(43) Zhang, H.; Banfield, J. F. *Nano Lett.* **2004**, *4*, 713.

Finally, for some particle size (which must be larger than 3 nm), the surface/bulk ratio is small enough to allow the formation of the sphalerite structure, which is the most stable crystal phase of ZnS. Ongoing calculations are focusing on these hypotheses in order to confirm this general view of the processes of nucleation and crystal growth of ZnS.

Further investigations reporting subsequent stages of aggregation will be reported shortly. In this study, we have employed only theoretical techniques. Experimental studies aimed at testing our predictions would clearly be desirable.

Acknowledgment. We would like to thank Alexey Sokol for his help and contributions. We also thank the EU for funding this work through the NUCLEUS project, and EPSRC for providing the computational resources.

Supporting Information Available: Additional graphs of Zn-S coordination at various concentrations; graph of S-O RDFs and coordination number of S^{2-} in solution. This material is available free of charge via the Internet at http://pubs.acs.org.

JA045274R